Validation of Shielding Effectiveness Measurement Method Using Nested Reverberation Chambers by Comparison with Aperture Theory

EMC Europe 2012, 11th International Symposium on EMC, Rome, Italy, 17-21 Sept., 2012 (ISSN: 2325-0356)

Citation for the published paper:
Carlsson, J. ; Karlsson, K. ; Johansson, A. (2012) "Validation of Shielding Effectiveness Measurement Method Using Nested Reverberation Chambers by Comparison with Aperture Theory". EMC Europe 2012, 11th International Symposium on EMC, Rome, Italy, 17-21 Sept., 2012

http://dx.doi.org/10.1109/EMCEurope.2012.6396716

Validation of Shielding Effectiveness Measurement Method Using Nested Reverberation Chambers by Comparison with Aperture Theory

Jan Carlsson, Kristian Karlsson
SP Technical Research Institute of Sweden
Box 857, SE-501 15 Borås, Sweden
jan.carlsson@sp.se, kristian.karlsson@sp.se

Andreas Johansson
Lund University
Box 118, SE-221 00 Lund, Sweden

***Abstract*—In this paper we revisit existing methods for measuring the shielding effectiveness of material samples using nested reverberation chambers. These methods have the advantage of exposing the sample with a more realistic environment than other methods that are based on single plane wave excitation. That is, in the reverberation chamber the sample is exposed to fields with different incidence directions and polarizations resulting in that the average shielding effectiveness can be measured. We show by comparison with aperture theory that the measured shielding effectiveness corresponds to the theoretical value. We show also by measurements that a corrugation or choke on the periphery of an aperture can be used for increasing the shielding effectiveness for a narrow frequency range.**

Shielding effectiveness; nested reverberation chambers; aperture attenuation; chokes; corrugations

I. INTRODUCTION

In EMC applications there is often a need for determining shielding properties for materials. Examples are materials for use in shielding gaskets, conductive meshes for use in displays and ventilation panels, composite materials and conductive paints for cases and housings for electronic equipment, to mention only a few. Normally we quantify the shielding properties in terms of the shielding effectiveness (SE) which is defined as the ratio of the transmitted power through the material to the incident power, i.e.,

$$\mathrm{SE}_{\mathrm{dB}} = -10\log_{10}\left(\frac{P_t}{P_i}\right) \tag{1}$$

where P_t is the transmitted power and P_i the incident power. In principle, SE can be determined either by numerical modeling or measurements. However, practical materials used for shielding purposes have often a structure that is very complex, and it might also be irregular. This requires a detailed numerical model which has the disadvantages of being difficult and time consuming to solve. Therefore is numerical modeling in general not a feasible method for determining the SE and measurements are consequently used instead.

Existing measurement techniques for determining the SE are normally designed to give SE for far-field conditions, i.e. the case of uniform plane wave incidence. There exist also methods that give SE for near-field conditions, such as the dual TEM cell method [1] but also other methods such as those discussed in [2]. In the present paper we consider only SE measurement methods for far-field conditions. The far-field measurement method in [3] is intended for characterizing shielding enclosures, but very often is the same methodology used also for measuring SE of material samples. Then the test sample is placed in an aperture in the enclosure and linearly polarized antennas are used to generate the incident power density as well as for measuring the power density on the other side of the test sample. The idea is to expose the test sample with a linearly polarized plane wave, and consequently only a limited set of incidence directions and polarizations can be tested in practice. There is therefore no guarantee that neither the minimum nor the maximum SE is found when using this kind of methods. It can also be argued that in real-life, equipment is seldom exposed to a single plane wave, instead some kind of multipath excitation is a more realistic scenario and therefore the average SE is the relevant measure. The average SE can be obtained by exciting the test sample with many plane waves with random incidence directions and polarizations, measure the power levels on both sides of the sample, repeating for a new set of incident waves a sufficient number of times and taking the average. As it turns out this is exactly what is done when using reverberation chamber methods.

The reverberation chamber is basically a cavity that is large in terms of the wavelength. Since it is large and the Q-value is finite we excite many modes at each frequency, and since each mode can be shown to correspond to up to eight plane waves [4] we have many plane waves coming from different directions and having different polarizations inside the chamber. Now, if we alter the mode configuration, e.g. by moving a metallic plate to a new position, we have created a new set of plane waves. If we do this a sufficient number of times, and the chamber is good, we are able to create a rich isotropic multipath environment with a well-defined average power level. In fact, the standard deviation of the average power level decreases as one over the square root of the number of independent samples, where each sample represents a power sample for a given stirrer position (assuming each position gives an independent sample). In a good chamber, we can quite easily achieve a standard deviation (2σ) better than

1 dB. By using a nested chamber configuration, e.g. by having one small chamber inside a bigger one, we can measure the average SE for a sample placed in an aperture in the small chamber. It should here be pointed out that in doing this we need to stir the modes in both chambers so that both the transmitted and the incident powers in (1) represent average power levels.

In this paper we revisit the nested reverberation chamber methods described in [5]-[6]. As is exemplified in [6] some currently used methods give for certain conditions a nonzero SE when performing a measurement without a sample in the test fixture. Of course, the SE should be zero without a sample and in order to get rid of this deficiency a modified approach is proposed in [6]. We show in this paper that the modified method presented in [6] gives not only the correct zero SE without a sample but also the correct value when we have a sample in the test fixture. We do this by comparing measured values for apertures of different sizes with calculations using aperture theory. A method for increasing the SE in a narrow frequency band by the use of corrugations or chokes is also presented.

II. Reverberation Chamber Measurement Methods

In Fig. 1 is shown the basic setup for measuring SE using nested reverberation chambers. In the outer chamber we use two antennas, one for injecting the power and the other for measuring the power level. Similarly, we use one antenna in the inner chamber for measuring the power level on the other side of the test sample. It is convenient to use a vector network analyzer (VNA) and connecting the transmitting antenna to port 1 and in turn the other two antennas to port 2. Then the SE is given by,

$$\mathrm{SE}_{\mathrm{dB}} = -10\log_{10}\left(\frac{\bar{P}_{ic,s}}{\bar{P}_{oc,s}}\right) = -20\log_{10}\left(\frac{\left|\bar{S}_{21,io,s}\right|}{\left|\bar{S}_{21,oo,s}\right|}\right) \qquad (2)$$

where the powers $P_{oc,s}$ and $P_{ic,s}$ are defined in Fig. 2, $S_{21,io,s}$ and $S_{21,oo,s}$ represent transmission from the transmitting antenna in the outer chamber to the receiving antennas in the inner and outer chamber, respectively. The subscript *s* denotes that the test sample is in place. The bars over the measured quantities denote ensemble averages obtained from a large number of stirrer positions, of the stirrers in both chambers.

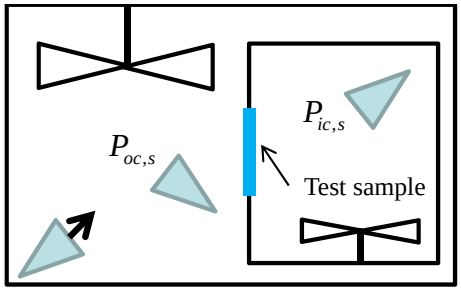

Figure 1. Basic nested reverberation chamber setup for measuring SE.

If we have no sample in the aperture in the inner chamber we expect to get a zero SE. In Fig. 2 is shown an example of measured SE without a sample, and as can be seen the basic method gives a non-zero SE.

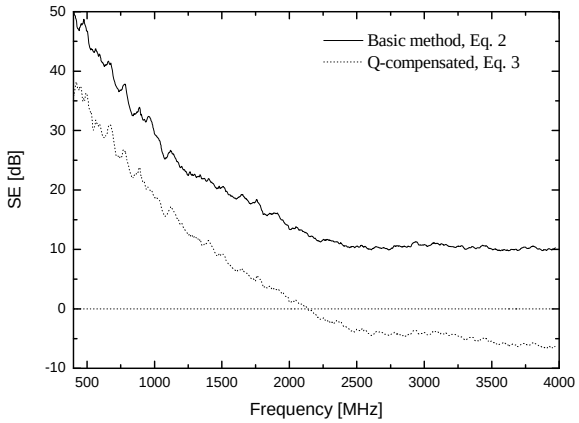

Figure 2. Examples of measured SE using basic and Q-compensated methods.

A. *Basic Method with Compensation for Q-factor in Inner Chamber*

Since the basic method might give a non-zero SE without a sample, it is in the standard [5] proposed to add a correction factor. Then the SE is given by,

$$\mathrm{SE}_{\mathrm{dB}} = -10\log_{10}\left(\frac{\bar{P}_{ic,s}}{\bar{P}_{oc,s}}\right) + \mathrm{CF}_{\mathrm{dB}} \qquad (3)$$

The correction factor in (3) is basically a compensation for the Q-factor in the inner chamber and is defined as,

$$\mathrm{CF}_{\mathrm{dB}} = 10\log_{10}\left(\frac{\bar{P}_{rQic,s}}{\bar{P}_{tQic,s}}\right) = 20\log_{10}\left(\left|\bar{S}_{21,ii,s}\right|\right) \qquad (4)$$

where the powers are defined in Fig. 3.

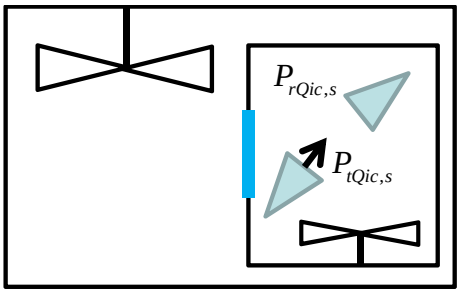

Figure 3. Setup for measuring the correction factor CF in (3).

As can be seen in Fig. 2 the addition of the correction factor changes the situation, but still we get a non-zero SE for the case without a sample. It should here be pointed out that the shortcomings of the two methods discussed so far are due to that these methods do not correctly account for aperture and cavity sizes and loading effects. This is recognized in the standard [5] and for cases when the methods fail the method discussed in the next section is recommended.

B. Method Proposed by Holloway et al. [6]

In [6] Holloway et al. derive a method that guarantees that the SE is zero without a sample. They show that the SE can be expressed as the ratio between two effective cross sections, one for the aperture in the inner chamber without the sample and the other with the sample in place. Thus, the SE is given by,

$$\mathrm{SE}_{\mathrm{dB}} = -10\log_{10}\left(\frac{\bar{\sigma}_s}{\bar{\sigma}_{ns}}\right) \tag{5}$$

where $\bar{\sigma}_{ns}$ and $\bar{\sigma}_s$ are the average cross sections without and with the sample in place, respectively. It is readily seen from (5) that the SE becomes zero with no sample since then $\bar{\sigma}_s = \bar{\sigma}_{ns}$. In order to measure SE according to (5) we need to measure the same power quotients as for the previously discussed methods but in addition also for the case without a sample in place. From [6] and using the same notation as defined in Fig. 1 and 3, the expression is,

$$\mathrm{SE}_{\mathrm{dB}} = -10\log_{10}\left(\frac{\bar{P}_{ic,s}}{\bar{P}_{ic,ns}}\frac{\bar{P}_{oc,ns}}{\bar{P}_{oc,s}}\frac{\bar{P}_{rQic,ns}}{\bar{P}_{tQic,ns}}\frac{\bar{P}_{tQic,s}}{\bar{P}_{rQic,s}}\right) \tag{6}$$

from which it also readily can be seen that the SE reduces to zero for the case of no sample. If we use a NVA and measure the S-parameters the expression reduces to,

$$\mathrm{SE}_{\mathrm{dB}} = -20\log_{10}\left(\frac{\left|\bar{S}_{21,io,s}\right|}{\left|\bar{S}_{21,io,ns}\right|}\frac{\left|\bar{S}_{21,oo,ns}\right|}{\left|\bar{S}_{21,oo,s}\right|}\frac{\left|\bar{S}_{21,ii,ns}\right|}{\left|\bar{S}_{21,ii,s}\right|}\right) \tag{7}$$

since the two last ratios in (6) are equal to $\left|\bar{S}_{21,ii,ns}\right|^2$ and $1\Big/\left|\bar{S}_{21,ii,s}\right|^2$, respectively. We know that this method gives the correct 0 dB SE when we have no sample, but still it remains to show that it gives the correct value also for other cases. This will be addressed in the following sections.

III. Attenuation in Apertures

In order to verify that the measurement method described in section II-B gives the correct SE we need to perform measurements on samples for which we can determine the SE with some other method. Our choice is to simply use circular apertures of different sizes for which we have theoretical formulas. As can be seen from (5) the SE is given by the ratio of two cross sections. The cross section $\bar{\sigma}_{ns}$ represents the aperture in the inner chamber when no test sample is mounted. In our measurement setup this is a quadratic aperture with a side length of 0.3 m, see section IV. The other cross section, $\bar{\sigma}_s$, represents the test sample and is in our case, as already mentioned, a circular aperture.

In general, aperture theory can be subdivided into three cases, when the aperture is small, comparable to, and large in terms of the wavelength. Here we will only consider the cases when the aperture is small and large in terms of the wavelength since for these cases we can find simple expressions for the cross section. For the intermediate region the theory becomes more complicated and we are normally forced to use numerical methods [7].

A. Apertures of Arbitrary Shape

When the aperture is electrically large we can use the geometrical optics approximation from which it is found that the cross section is independent of frequency, polarization and azimuth of the incident field. It is however a function of the incident elevation angle but since we here are only interested in the average cross section this dependence is averaged out and the expression becomes [8],

$$\bar{\sigma} = A/2 \tag{8}$$

where A is the aperture area.

When the aperture is electrically small we can use polarizability theory [7], [9] which states that the transmitted field can be determined as the fields from electric and magnetic dipole moments. It can be shown that the cross section has the following frequency dependence,

$$\bar{\sigma} = Cf^4 \tag{9}$$

where C is a constant that depends on the aperture size and shape.

B. Circular Aperture

By using (8) the cross section for an electrically large circular aperture can be written as,

$$\bar{\sigma} = \pi a^2/2 \tag{10}$$

where a is the radius of the aperture. For an electrically small circular aperture it is possible to find the constant C in (9), the result is [7]-[9],

$$\bar{\sigma} = \frac{16a^6}{9\pi}\left(\frac{2\pi f}{c_0}\right)^4 \tag{11}$$

where c_0 is the speed of light in vacuum (or in the media filling the aperture).

In fact, it is also possible to find analytical expressions for the intermediate frequency region for circular apertures, but we will not pursue this here. Instead we will for simplicity use (10) and (11).

C. Corrugations to Increase SE

As can be seen from (8) the cross section will for high frequencies be determined by the physical aperture area and is constant. This means that the SE will be constant, and for EMC applications the value will often be too low. It is therefore of interest to be able to increase the SE in some way. One idea is to provide a soft boundary condition [10]-[11] around the periphery of the aperture. This can be realized by the use of a corrugation or choke as shown in Fig. 4. This is similar to what was shown to work well for a circular waveguide feedthrough in [12] and for slots in [13].

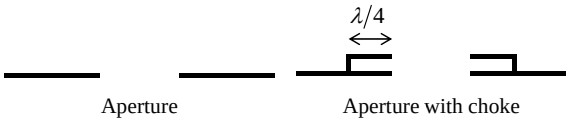

Figure 4. Aperture without and with corrugation (choke).

IV. Measurement Setup

For the measurements we used a small reverberation chamber with the dimensions 0.85 by 1.2 by 1.2 m that was placed inside another chamber with the dimensions 2.5 by 2.5 by 3.1 m. The test sample is placed in a square aperture with the size 0.3 by 0.3 m. This aperture is placed in one of the walls of the inner chamber, see Fig. 5.

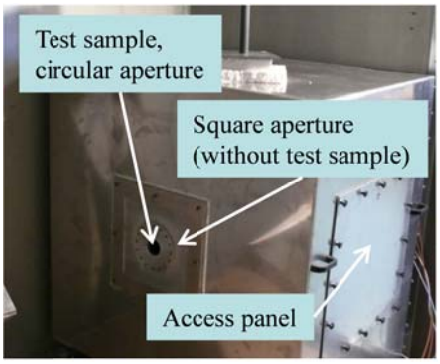

Figure 5. Picture of the inner chamber with a circular aperture as test sample.

In the outer chamber we have two metallic stirrers that are rotated in discrete steps, in the inner chamber the single stirrer is rotating continuously, see Fig. 6.

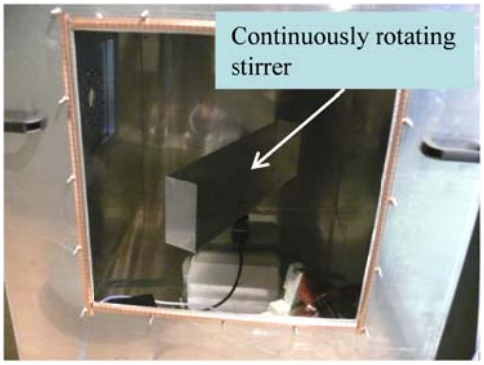

Figure 6. Inner chamber with the stirrer seen through the access panel.

When using a continuously rotating stirrer care should be taken so that the rotation speed does not affect the measurement results. We checked this by changing the speed within the possibilities of the motor and did not see any influence. For the measurements we used a speed of about 20 rpm for the stirrer in the inner chamber. In the outer chamber 8 steps were used for one of the stirrers and 30 for the other, giving a total of 240 samples. In addition we used frequency stirring corresponding to a bandwidth of approximately 50 MHz. With the given dimensions for the chambers we are able to measure down to approximately 500 MHz.

V. Results

In order to verify the measurement method discussed in section II-B we measured the SE for five different circular apertures with radii ranging from 7.5 to 120 mm. The measured values are then compared to theoretical values obtained by using (10) and (11) for high and low frequencies, respectively. It should be noted that the measured SE actually is a ratio of two cross sections, one for the test sample and the other for the case without test sample (i.e. the square aperture), according to (5). Thus, we have in the following plots corrected the theoretical values with the cross section for the square aperture to get the SE.

In Fig. 7 is shown the SE for the three largest apertures that were measured. It can be noted that the largest circular aperture with the radius 120 mm can be considered large in terms of the wavelength in the whole frequency range 500 MHz – 4 GHz since it has an almost constant SE (and consequently cross section). It can therefore be concluded that the square aperture, which is even larger with the dimension 0.3 by 0.3 m, also can be considered large in the whole frequency range so it has a constant cross section that is given by half its physical area, see (8). This is the value we have used for correcting the theoretical cross sections to get the SE.

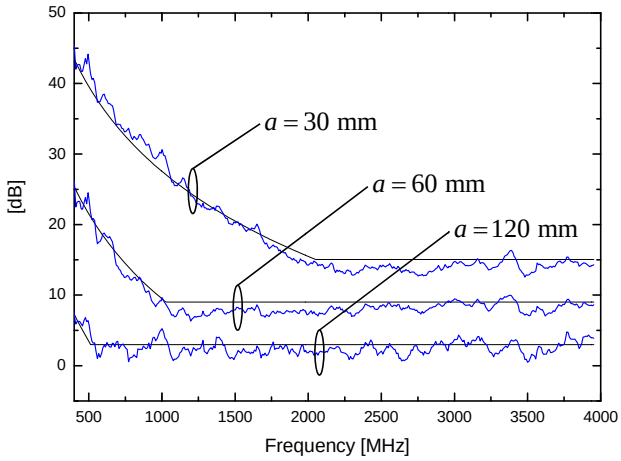

Figure 7. Measured SE for circular apertures with radii 30, 60 and 120 mm, respectively. Solid black lines represent theoretical values.

As can be seen in Fig. 7 we have a good agreement between measured and theoretical values in the whole frequency range. It is however somewhat surprising that we have so good agreement also in the intermediate frequency range where the high and the low frequency approximations (10) and (11), respectively are strictly not valid.

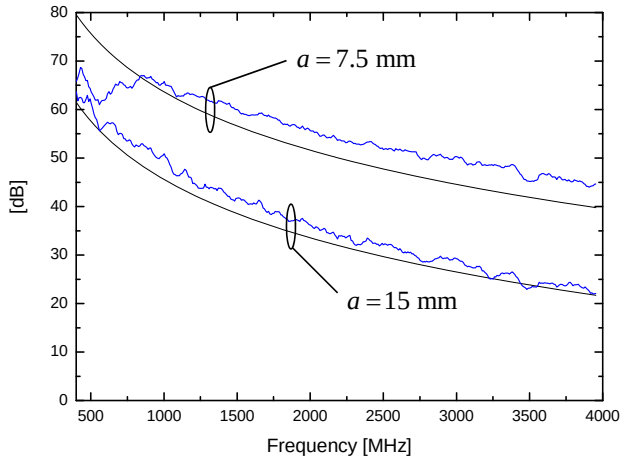

Figure 8. Measured SE for circular apertures with radii 7.5 and 15 mm, respectively. Solid black lines represent theoretical values.

Fig. 8 shows the SE for the two smallest apertures. As can be observed both apertures are small in terms of the wavelength in the whole frequency range since the SE decreases with frequency in the whole range. It can also be observed that the agreement is not as good as before, and the agreement is worse for the aperture with the smaller radius. This can be explained by that the aperture theory presented in section III is strictly valid for apertures in infinitesimally thin planes. For the measurements the apertures were made in aluminum plates with a thickness of 3 mm. This explanation is proved in Fig. 9 where the smallest aperture is measured also for a plate with a thickness of 1 mm. The agreement becomes better for the thinner plate. As also can be seen in Fig. 8 we have problems with the dynamic range for the smallest aperture and low frequencies, the SE flattens out as it should not do. However, we made no attempt to approve the dynamic range by e.g. using an amplifier.

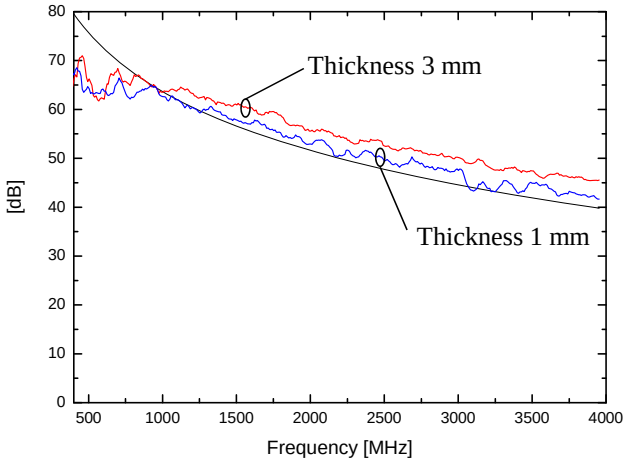

Figure 9. Measured SE for circular aperture with radius 7.5 mm and depth 1 and 3 mm, respectively. Solid black line represents theoretical values.

In order to test if a corrugation or choke around the periphery of a circular aperture (see section III-C) would give an increase of the SE close to the design frequency we manufactured a test sample and performed a measurement. The design frequency is 3.26 GHz corresponding to a corrugation depth of 23 mm. The width of the corrugation was selected to be 24 mm and the radius of the circular aperture was 60 mm. The measured result is shown in Fig. 10 and as can be seen the SE is increased close to the design frequency. The gain in SE is about 15 dB but it should be possible to gain more by cascading several corrugations. It should also be possible to make it more broadband by cascading several corrugations with different depths.

The reason for the increase in SE for low frequencies is the added depth to the circular aperture. We verified this by short circuiting the corrugation with copper tape, although this measurement is not shown in Fig. 10.

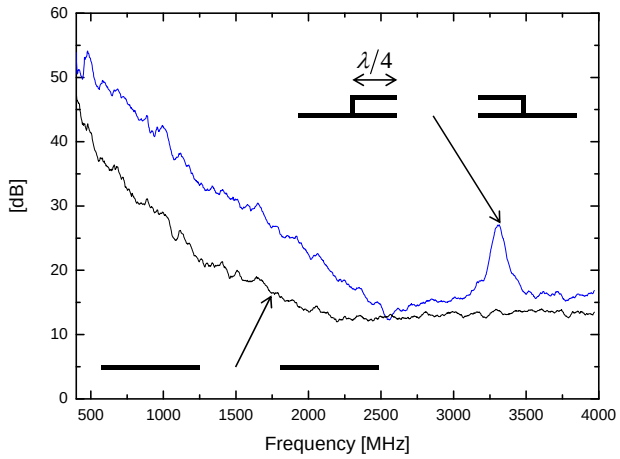

Figure 10. Measured SE for circular aperture with radius 60 mm with and without corrugation, respectively.

VI. Conclusions

We have measured the average SE for five circular apertures with radii in the range 7.5 to 120 mm by using the nested reverberation chamber method proposed by Holloway et al. in [6]. The agreement between measured values and those obtained by the use of aperture theory was found to be very good. The discrepancies for small apertures were found to be due to the finite thickness of the metallic plates in which the apertures were made. By using a thinner plate the agreement between measured and calculated values became better.

From this we draw the conclusion that the method proposed in [6] gives the correct SE, not only for the case without a sample as was already shown in [6] but also for real samples.

We also showed by an example that it is possible to increase the SE in a narrow frequency range by using corrugations around the periphery of the aperture. Although only shown for a circular aperture it should be applicable also for apertures with other shapes.

References

[1] P. F. Wilson, and M. T. Ma, "Shielding-Effectiveness Measurements with a Dual TEM Cell", *IEEE Trans. Electromagn. Compat.*, vol. EMC-27, no. 3, pp. 137-142, Aug. 1985.

[2] —, “Techniques for Measuring the Electromagnetic Shielding Effectiveness of Materials: Part II – Near-Field Source Simulation”, *IEEE Trans. Electromagn. Compat.*, vol. 30, no. 3, pp. 137-142, Aug. 1988.

[3] IEEE-STD-299, “Standard Method for Measuring the Effectiveness of Electromagnetic Shielding Enclosures”, IEEE, Piscataway, NJ, 1997.

[4] K. Rosengren, and P.-S. Kildal, “Study of Distributions of Modes and Plane Waves in Reverberation Chambers for Characterization of Antennas in Multipath Environment”, Microwave and Optical Technology Letters, vol. 30, no. 20, pp. 386-391, Sept. 2001.

[5] IEC 61000-4-21, “Electromagnetic compatibility (EMC) – Part 4-21: Testing and measurement techniques – Reverberation chamber test methods”, First edition 2003-08.

[6] C. L. Holloway, D. A. Hill, J. Ladbury, G. Koepke, and R. Garzia, “Shielding Effectiveness Measurements of Materials Using Nested Reverberation Chambers”, *IEEE Trans. Electromagn. Compat.*, vol. 45, no. 2, pp. 350-356, May 2003.

[7] C. M. Butler, Y. Rahmat-Samii, and R. Mittra, “Electromagnetic Penetration Through Apertures in Conducting Surfaces”, *IEEE Trans. Antennas Propagat.*, vol. AP-26, no. 1, pp. 82-93, Jan. 1978.

[8] D. A. Hill, M. T. Ma, A. R. Ondrejka, B. F. Riddle, M. L. Crawford, and R. T. Johnk, “Aperture Excitation of Electrically Large, Lossy Cavities”, *IEEE Trans. Electromagn. Compat.*, vol. 36, no. 3, pp. 169-178, Aug. 1994.

[9] H. A. Bethe, “Theory of Diffraction by Small Holes”, *Phys. Rev.*, vol. 66, pp. 163-182, 1944.

[10] P.-S. Kildal, “Definition of artificially soft and hard surfaces for electromagnetic waves”, *Electron. Lett.*, vol. 24. no. 3, pp. 168-170, Feb. 1988.

[11] P.-S. Kildal, “Artificially soft and hard surfaces in electromagnetics”, *IEEE Trans. Antennas Propagat.*, vol. 38, no. 10, pp. 1537-1544, Oct. 1990.

[12] J. Carlsson, L. Fast, C. Karlsson, “The use of Corrugations to Enhance Shielding Effectiveness of Fiber Optic Waveguide Feedthrough”, EMC Europe 2010, 9th International Symposium on EMC, Wroclaw, Poland, 13-17 Sept., 2010.

[13] J. Carlsson, and P.-S. Kildal, “Transmission Through Corrugated Slots”, *IEEE Trans. Electromagn. Compat.*, vol. 37, no. 1, pp. 114-121, Feb. 1995.